Modelling Surface Acoustic Wave Driven Thin Film Flows over Topography

Bhargav Samineni

May 11, 2022

Abstract

Motivated by the acoustowetting phenomenon and its applications to the dynamic wetting of objects by a coating liquid, we explore the influence of surface acoustic waves and gravity on the motion of a thin film flowing over a surface. We consider surfaces that may be both inclined and include topographical features like trenches, mounds, bumps, etc. Using the lubrication approximation, we reduce the equations of motion for the film to a single nonlinear partial differential equation that describes the evolution of the film height relative to the surface topography in time and space.

1 Introduction

The motion of thin liquid films with fronts is a relatively ubiquitous dynamic in nature that also has applications to a number of technical fields and processes. Particularly with respect to coating processes, the influence of other factors besides viscous and surface tension forces (such as gravity [DK02] and electric fields [Ver+12]) has also been studied. Recent experiments have shown that high frequency surface acoustic waves may be a novel method for coating techniques, particularly between two liquids where one of the liquids is not influenced by the acoustic streaming, so in this report we study the affect of these acoustic waves on the dynamics of thin liquid films. Specifically, we approach the problem using the lubrication approximation to reduce the Navier-Stokes equations into a single nonlinear PDE and simplify the interactions between the two liquids by considering the stationary one to be a topographical feature of our surface. Both the influence of surface acoustic waves on the spreading of liquid films (see [AM16]) and coating over topography with gravity as the primary driving have been previously studied (see [KBH00; SL88; Ver11]), but to the best of our knowledge the intersection of these two interactions has not been studied.

2 Governing Equation

We let $s(x, y)$ describe the topography of the surface, $h(x, y, t)$ be the film thickness relative to $s(x, y)$ at any point in the (x, y) plane at a time t, and $\phi(x, y, t) = s(x, y) + h(x, y, t)$ be the height of the free surface at any point in the (x, y) plane at a time t. We consider both the influence of gravity and acoustic streaming on the motion of the film, so our surface may also be inclined in addition to having Rayleigh surface acoustic waves (SAWs) propagating along the x-coordinate as shown in Fig. 1.

The starting point for modeling thin films are the incompressible Navier-Stokes equations

$$\nabla \cdot \boldsymbol{u} = 0 \tag{1}$$

$$\rho\left(\frac{\partial \boldsymbol{u}}{\partial t} + (\boldsymbol{u}\cdot\nabla)\,\boldsymbol{u}\right) = -\nabla p + \mu\nabla^2\boldsymbol{u} + \rho g\sin\beta\boldsymbol{i} - \rho g\cos\beta\boldsymbol{k} - \rho J e^{2k_i(x+\alpha_1 z)}\boldsymbol{i} - \rho J\alpha_1 e^{2k_i(x+\alpha_1 z)}\boldsymbol{k} \tag{2}$$

where $\boldsymbol{u} = (u, v, w)$ is the fluid velocity, p is the fluid pressure, ρ is the fluid density, μ is the fluid viscosity k_i is the attenuation coefficient of the liquid, α_1 is the geometric constant of the liquid, and $J = \left(1 + \alpha_1^2\right) A^2\omega^2 k_i$ is a constant we define to consolidate terms from acoustic streaming. We refer to [SM94] for more information on acoustic streaming and the derivation of the equations for acoustic forcing.

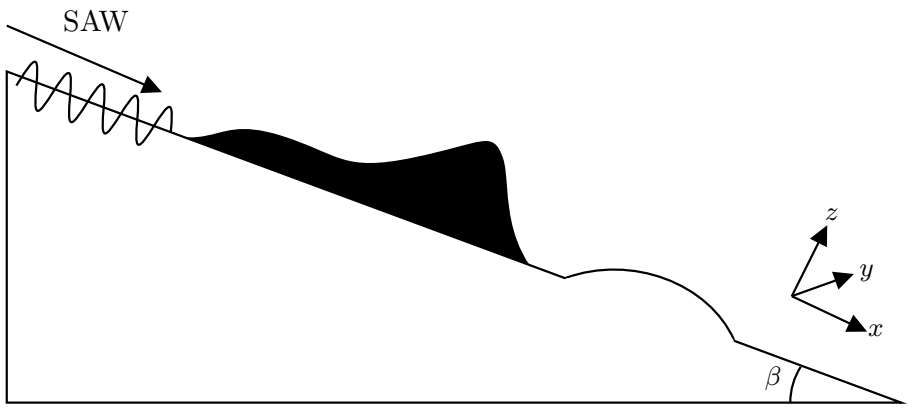

Figure 1: A simplified sketch of a fluid flowing down a plane inclined at an angle β. The SAW travels from left to right, and the surface of the plane is described by a topography function s that has a bump.

2.1 Lubrication Approximation

As shown in [Kon03], if the Reynold's number is sufficiently low, the inertial terms of the Navier-Stokes equations as well as the in plane derivatives and normal component of $\boldsymbol{u}$ can be ignored. Thus, under the effects of gravity and surface acoustic wave streaming forces, the lubrication approximation simplifies Eq. (2) to

$$\nabla_2 p = \mu \frac{\partial^2 \boldsymbol{v}}{\partial z^2} + \rho g \sin\beta \boldsymbol{i} - \rho J e^{2k_i(x+\alpha_1 z)} \boldsymbol{i} \tag{3}$$

$$\frac{\partial p}{\partial z} = -\rho g \cos\beta - \rho J \alpha_1 e^{2k_i(x+\alpha_1 z)} \tag{4}$$

where $\nabla_2 = (\partial_x, \partial_y)$ and $\boldsymbol{v} = (u, v)$.

2.2 Boundary Conditions

The Laplace-Young boundary condition states that at the interface $z = \phi(x, y, t)$, the pressure is given by $p(\phi) = -\gamma\kappa + p_0$, where κ is the curvature of the boundary, γ is the surface tension, and p_0 is the atmospheric pressure. Thus, integrating Eq. (4) gives

$$\begin{aligned}
\int_\phi^z \frac{\partial p}{\partial z}\, dz &= \int_\phi^z -\rho g \cos\beta - \rho J \alpha_1 e^{2k_i(x+\alpha_1 z)}\, dz \\
p(z) - p(\phi) &= -(z-\phi)\rho g \cos\beta - \frac{\rho J}{2k_i}\left(e^{2k_i(x+\alpha_1 z)} - e^{2k_i(x+\alpha_1\phi)}\right) \\
p(z) &= -(z-\phi)\rho g \cos\beta - \frac{\rho J}{2k_i}\left(e^{2k_i(x+\alpha_1 z)} - e^{2k_i(x+\alpha_1\phi)}\right) - \gamma\kappa + p_0.
\end{aligned} \tag{5}$$

If we define $P(x, y, t) = \phi\rho g \cos\beta + \frac{\rho J}{2k_i} e^{2k_i(x+\alpha_1\phi)} - \gamma\kappa$, this simplifies Eq. (5) to

$$p(z) = P - z\rho g \cos\beta - \frac{\rho J}{2k_i} e^{2k_i(x+\alpha_1 z)} + p_0$$

which further gives

$$\nabla_2 p = \nabla_2 \left(P - \frac{\rho J}{2k_i} e^{2k_i(x+\alpha_1 z)}\right) = \nabla P - \rho J e^{2k_i(x+\alpha_1 z)} \boldsymbol{i}. \tag{6}$$

Further boundary conditions include

$$\boldsymbol{v}\big|_{z=s(x,y)} = \mathbf{0} \tag{7}$$

$$\frac{\partial \boldsymbol{v}}{\partial z}\Big|_{z=\phi(x,y,t)} = \mathbf{0} \tag{8}$$

where Eq. (7) is a no-slip boundary condition along the surface $z = s(x, y)$ and Eq. (8) enforces vanishing shear stresses along the fluid-air boundary $z = \phi(x, y, t)$.

2.3 Film Equation

Using the Laplace-Young boundary condition and substituting Eq. (6) into Eq. (3) yields

$$\nabla P = \mu \frac{\partial^2 \boldsymbol{v}}{\partial z^2} + \rho g \sin\beta \boldsymbol{i}. \tag{9}$$

Integrating Eq. (9) twice with respect to z and utilizing the boundary conditions in Eq. (7) and Eq. (8) gives

$$\begin{aligned}
\int_s^z \int_z^\phi \frac{\partial^2 \boldsymbol{v}}{\partial z^2}\, dz dz &= \frac{1}{\mu}\int_s^z \int_z^\phi \left(\nabla P - \rho g \sin\beta \boldsymbol{i}\right)\, dz dz \\
\int_s^z \frac{\partial \boldsymbol{v}}{\partial z}\, dz &= \frac{1}{\mu}\left(\nabla P - \rho g \sin\beta \boldsymbol{i}\right)\int_s^z (z-\phi)\, dz \\
\boldsymbol{v} &= \frac{1}{\mu}\left(\nabla P - \rho g \sin\beta \boldsymbol{i}\right)\left(\frac{z^2}{2} - \phi z - \frac{s^2}{2} + \phi s\right).
\end{aligned} \tag{10}$$

Averaging over the height removes the z dependence of $\boldsymbol{v} = (u, v)$ and gives the equation $\overline{\boldsymbol{v}} = \frac{1}{h}\int_s^\phi \boldsymbol{v}\, dz$. Plugging in Eq. (10) and solving this integral then gives

$$\begin{aligned}
\overline{\boldsymbol{v}} &= \frac{1}{h}\int_s^\phi \frac{1}{\mu}\left(\nabla P - \rho g \sin\beta \boldsymbol{i}\right)\left(\frac{z^2}{2} - \phi z - \frac{s^2}{2} + \phi s\right)\, dz \\
&= \frac{1}{\mu h}\left(\nabla P - \rho g \sin\beta \boldsymbol{i}\right)\left(-\frac{\phi^3}{3} + \phi^2 s - \phi s^2 + \frac{s^3}{3}\right) \\
&= -\frac{h^2}{3\mu}\left(\nabla P - \rho g \sin\beta \boldsymbol{i}\right).
\end{aligned} \tag{11}$$

The conservation of mass, when depth-averaged, gives $\frac{\partial h}{\partial t} + \nabla \cdot (h\overline{\boldsymbol{v}}) = 0$ which results in

$$\begin{aligned}
\frac{\partial h}{\partial t} &= \frac{1}{3\mu}\nabla \cdot \left[h^3\left(\nabla P - \rho g \sin\beta \boldsymbol{i}\right)\right] \\
&= \frac{1}{3\mu}\nabla \cdot \left[h^3\left(\rho g \cos\beta \nabla\phi - \gamma \nabla\kappa - \rho g \sin\beta \boldsymbol{i} + \frac{\rho J}{2k_i}\nabla e^{2k_i(x+\alpha_1\phi)}\right)\right].
\end{aligned} \tag{12}$$

when plugging in Eq. (11). Approximating the curvature $\kappa \approx \nabla^2\phi$ then gives

$$\begin{aligned}
\frac{\partial h}{\partial t} &= \frac{1}{3\mu}\nabla \cdot \left[h^3\left(\rho g \cos\beta \nabla\phi - \gamma \nabla\nabla^2\phi - \rho g \sin\beta \boldsymbol{i} + \frac{\rho J}{2k_i}\nabla e^{2k_i(x+\alpha_1\phi)}\right)\right] \\
&= \frac{1}{3\mu}\left[\nabla \cdot \left[\rho g \cos\beta h^3 \nabla\phi\right] - \nabla \cdot \left[\gamma h^3 \nabla\nabla^2\phi\right] - \rho g \sin\beta \frac{\partial h^3}{\partial x} + \nabla \cdot \left[\frac{\rho J}{2k_i} h^3 \nabla e^{2k_i(x+\alpha_1\phi)}\right]\right].
\end{aligned} \tag{13}$$

2.4 Dimensionless Form

We scale the in-plane coordinates and time by

$$\overline{x} = \frac{x}{x_c}, \quad \overline{y} = \frac{y}{x_c}, \quad \overline{z} = \frac{z}{h_c}, \quad \overline{t} = \frac{t}{t_c}$$

where an overline denotes a non-dimensional quantity. Substituting these scales into Eq. (13) and removing any overlines gives

$$\frac{h_c}{t_c}\frac{\partial h}{\partial t} = \frac{1}{3\mu}\left[\frac{h_c^4}{x_c^2}\rho g\cos\beta\nabla\cdot\left[h^3\nabla\phi\right] - \frac{\gamma h_c^4}{x_c^4}\nabla\cdot\left[h^3\nabla\nabla^2\phi\right] - \frac{h_c^3}{x_c}\rho g\sin\beta\frac{\partial h^3}{\partial x}\right] + \frac{1}{3\mu}\left[\frac{\rho J^* h_c^3}{2x_c^2}\nabla\cdot\left[h^3\nabla e^{2k_i(x+\alpha_1\phi(h_c/x_c))}\right]\right] \tag{14}$$

where $J^* = \left(1+\alpha_1^2\right)A^2\omega^2$. By virtue of the fact that we are looking at thin films, we define $\varepsilon = h_c/x_c$ where $h_c \ll x_c$. This gives

$$\frac{h_c}{t_c}\frac{\partial h}{\partial t} = \frac{1}{3\mu}\left[\frac{h_c^4}{x_c^2}\rho g\cos\beta\nabla\cdot\left[h^3\nabla\phi\right] - \frac{\gamma h_c^4}{x_c^4}\nabla\cdot\left[h^3\nabla\nabla^2\phi\right] - \frac{h_c^3}{x_c}\rho g\sin\beta\frac{\partial h^3}{\partial x} + \frac{\rho J^* h_c^3}{2x_c^2}\nabla\cdot\left[h^3\nabla e^{2k_i(x+\alpha_1\varepsilon\phi)}\right]\right],$$

which can be further manipulated to the form

$$\frac{\partial h}{\partial t} = \frac{\gamma h_c^3 t_c}{3\mu x_c^4}\left[\frac{x_c^2\rho g}{\gamma}\cos\beta\nabla\cdot\left[h^3\nabla\phi\right] - \nabla\cdot\left[h^3\nabla\nabla^2\phi\right] - \frac{x_c^3\rho g}{\gamma h_c}\sin\beta\frac{\partial h^3}{\partial x} + \frac{\rho J^* x_c^2}{2\gamma h_c}\nabla\cdot\left[h^3\nabla e^{2k_i(x+\alpha_1\varepsilon\phi)}\right]\right].$$

Choose t_c such that

$$t_c = \frac{3\mu x_c^4}{\gamma h_c^3}.$$

Additionally, we define the Bond number $\mathrm{Bo} = x_c^2\rho g/\gamma$ and acoustic Weber number $\mathrm{We_{ac}} = \rho\omega^2 A^2 x_c/\gamma$. Substituting these constants and expanding J^* yields a final equation

$$\frac{\partial h}{\partial t} = \mathrm{Bo}\cos\beta\nabla\cdot\left[h^3\nabla\phi\right] - \nabla\cdot\left[h^3\nabla\nabla^2\phi\right] - \frac{\mathrm{Bo}}{\varepsilon}\sin\beta\frac{\partial h^3}{\partial x} + \frac{\left(1+\alpha_1^2\right)\mathrm{We_{ac}}}{2\varepsilon}\nabla\cdot\left[h^3\nabla e^{2k_i(x+\alpha_1\varepsilon\phi)}\right]. \tag{15}$$

The first term and third terms represent the out of plane and in plane influences of gravity, respectively, on the film while the second term represents the influence of capillary forces and the fourth term represents the contribution of SAW driving.

2.5 Two-Dimensional Equation and Enforcing a Film Front

Although Eq. (15) is a simplified partial differential equation, it is still strongly nonlinear. To gain a basic understanding of some of its solutions, we make the further simplification that the free surface of the thin film does not change in the transverse direction (i.e. h and s are both y-independent). This assumption further reduces our problem to only one variable in space and simplifies Eq. (15) to

$$\frac{\partial h}{\partial t} = \mathrm{Bo}\cos\beta\left[h^3\phi_x\right]_x - \left[h^3\phi_{xxx}\right]_x - \frac{\mathrm{Bo}}{\varepsilon}\sin\beta\left[h^3\right]_x + \frac{k_i\left(1+\alpha_1^2\right)\mathrm{We_{ac}}}{\varepsilon}\left[h^3 e^{2k_i(x+\alpha_1\varepsilon\phi)}\left(1+\alpha_1\varepsilon\phi_x\right)\right]_x \tag{16}$$

where h and ϕ are now functions of x and t.

Additionally, to enforce that the SAW forcing occurs starting from the film front, we redefine k_i (in dimensionless form) as

$$k_i(\phi) = x_c\left(\left(k_i^{\mathrm{oil}} - k_i^{\mathrm{air}}\right)\left(1 - e^{-x_c(\phi-b)/\lambda}\right) + k_i^{\mathrm{air}}\right) \tag{17}$$

where k_i^{oil} denotes the attenuation in the film and k_i^{air} denotes the attenuation outside the film. The λ term is a dimensional constant that controls the steepness of the change from k_i^{air} to k_i^{oil}, while b denotes the precursor film height. In essence, when $\phi = b$, $k_i = x_c k_i^{\mathrm{air}}$ and decays to $x_c k_i^{\mathrm{oil}}$ as h increases. See Fig. 2 for an example of such a graph.

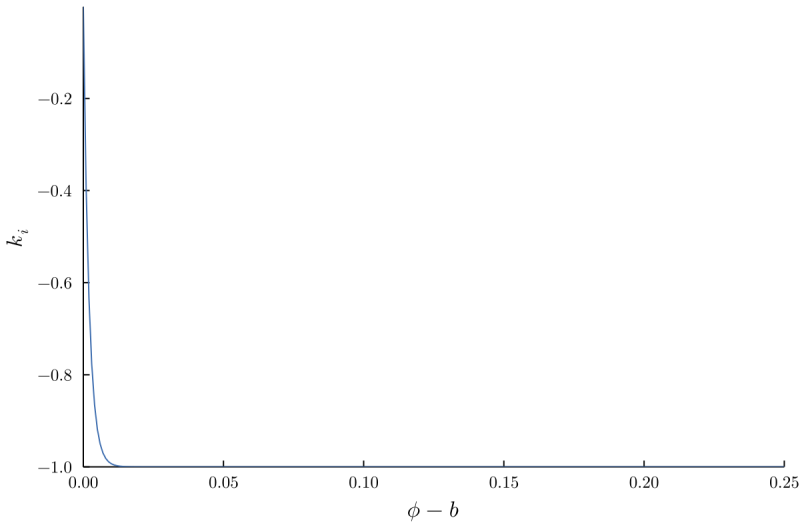

Figure 2: Attenuation as a function of ϕ for $k_i^{\text{oil}} = -1000\left[m^{-1}\right], k_i^{\text{air}} = -1\left[m^{-1}\right]$, $\lambda = 2 * 10^{-3}\,[m]$, and $x_c = 10^{-3}$.

3 Method of Solution

3.1 Spatial Discretization

If we define the domain of interest as $[0, L_x]$, we can discretize the domain into points $x_j = j\Delta x$ for $j = 0, \ldots, N_x$ where $\Delta x = L_x/N_x$ and N_x is the number of grid points excluding the origin. If we further define $h_j(t) = h(x_j, t)$, we can discretize Eq. (16) into a system of ordinary differential equations of the form

$$\frac{dh_j}{dt} = f_j = \text{Bo}\cos\beta f_j^{(1)} - f_j^{(2)} - \frac{\text{Bo}}{\varepsilon}\sin\beta f_j^{(3)} + \frac{k_i\left(1+\alpha_1^2\right)\text{We}_{\text{ac}}}{\varepsilon} f_j^{(4)}, \quad j = 1, \ldots, N_x - 1 \tag{18}$$

where $f_j^{(k)}$ is the discretization of the k-th term in the right-hand side of Eq. (16) and the ODEs for $j = 0, N_x$ are prescribed by boundary conditions. Because the governing equation contains high order derivatives, the discretization used for certain components needs special attention in order to not lead to a large computational stencil.

3.1.1 Fourth-Order Term

Following the method outlined in [Kon03], discretizing the fourth order term (i.e. $f_j^{(2)}$) can be done by a combination of forward and backward differences. If we define

$$h_{x,j} = \frac{h_{j+1} - h_j}{\Delta x} \qquad h_{\overline{x},j} = \frac{h_j - h_{j-1}}{\Delta x}$$

as the forward and backward differences, respectively, then a possible discretization is

$$f_j^{(2)} = \left(a(h_{j-1}, h_j)\,\phi_{\overline{x}x\overline{x},j}\right)_{x,j} \tag{19}$$

where $a(j_1, j_2) = \frac{1}{2}\left({j_1}^3 + {j_2}^3\right)$. This discretization leads to a second order approximation that has a five point stencil, which is better than the seven point stencil that would result from using a central differencing scheme.

3.1.2 Lower Order Terms

Because the other terms are lower order, we can apply simpler differencing methods as long as they are also second order and don't increase the size of the stencil. For example, we could apply a combination of forward

and backward differencing to get

$$f_j^{(1)} = \left(a(h_{j-1}, h_j)\, \phi_{x,j}\right)_{\overline{x},j}. \tag{20}$$

If we define central differencing as

$$h_{x^*,j} = \frac{h_{j+1} - h_{j-1}}{2\Delta x}$$

then the other two terms could be discretized as

$$f_j^{(3)} = \left(h_j^3\right)_{x^*,j} \tag{21}$$

$$f_j^{(4)} = \left(h_j^3 e^{2k_i(x_j + \alpha_1 \varepsilon \phi_j)} \left(1 + \alpha_1 \varepsilon \phi_{x^*,j}\right)\right)_{x^*,j}. \tag{22}$$

A complete expansion of these discretized terms is provided in Section B of the appendix.

3.2 Time stepping

Because the governing PDE describing the system is stiff (i.e. some numerical methods will be unstable unless the step size taken for time evolution is extremely small), we find that using explicit schemes do not work for time stepping. Thus, we choose to use an implicit scheme called Rodas4 implemented in the DifferntialEquations.jl library in Julia.

4 Numerical Simulations

While we have developed equations to model the influence of both SAWs and gravity on the motion of thin films, we are primarily concerned with the case where the SAW is the primary driving force. Hence, for all the simulations shown in this section we use $\beta = 0$. We also use the physical characteristics shown in Table 1, a precursor film height of $b = 0.01$, as well as a drop initial condition for all the simulations.

Parameter Values		
Symbol	Physical Meaning	Quantitative Value
ρ	Density of Oil	$900\ \left[\frac{Kg}{m^3}\right]$
g	Gravity	$9.8\ \left[\frac{m}{s^2}\right]$
μ	Dynamic Viscosity of Oil	$0.45\ \left[\frac{Kg}{ms}\right]$
γ	Surface Tension	$20 \times 10^{-3}\ \left[\frac{Kg}{s^2}\right]$
A	Amplitude of SAW	$8 \times 10^{-10}\ [m]$
ω	Angular Frequency of SAW	$2\pi \times 20 \times 10^6\ \left[s^{-1}\right]$
α_1	Geometric Constant	2.386
k_i^{oil}	Attenuation Coefficient in Oil	$-1000\ \left[m^{-1}\right]$
k_i^{air}	Attenuation Coefficient in Air	$-1\ \left[m^{-1}\right]$
λ	Steepness of Attenuation Coefficient Change	$2 \times 10^{-3}\ [m]$
h_c	Characteristic Film Thickness	$200 \times 10^{-6}\ [m]$
x_c	Characteristic Length Scale	$10^{-3}\ [m]$
t_c	Characteristic Time Scale	$.84375\ [s]$
ε	Small Parameter	0.2
Bo	Bond Number	0.441
We_{ac}	Acoustic Weber Number	0.45479

Table 1: Physical parameters and their values used in our simulations

4.1 Flat Topography

In this simulation we consider the scenario where we have a flat topography (i.e. $s(x) = 0$). This corresponds to a single initial drop being moved by SAW forcing with no other liquids in its path. We see in Fig. 3 that the initial oil drop moves from left to right and spreads out as it does so, which is consistent with experimental observations. We also note the formation of a capillary ridge near the contact line between the oil and the surface, which is also consistent with experimental observations.

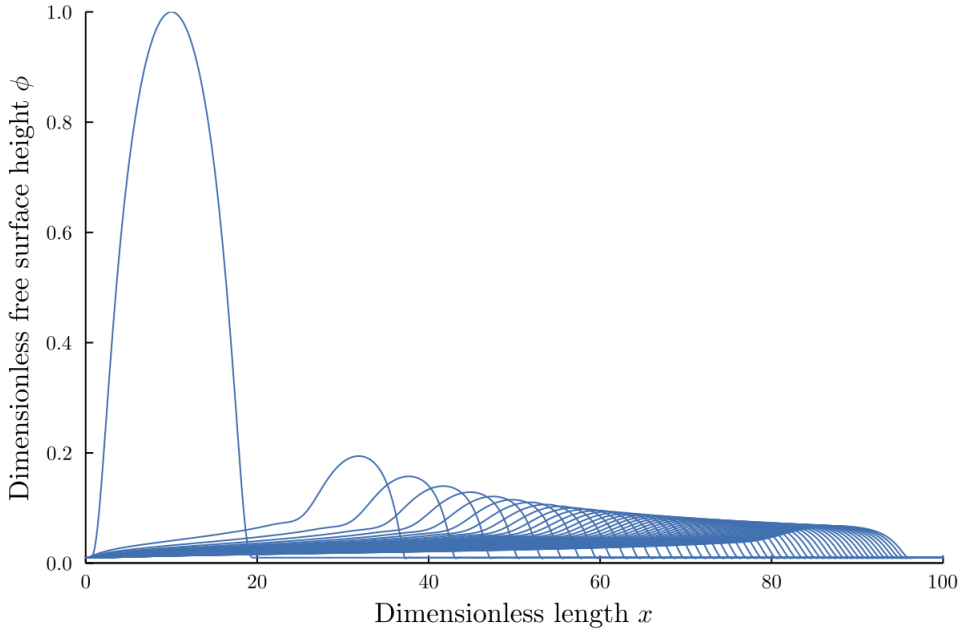

Figure 3: Fluid profile on a flat topography plotted every $\Delta t = 10000$ dimensionless time units

4.2 Bump Topography

In the following simulations we consider the scenario where we have a bump topography (see Section A in the appendix for a general bump equation). This corresponds to a single initial drop being moved by SAW forcing with another liquid in its path being modelled by the stationary bump. In the case where the maximum height of our bump is small, we find that the initial oil drop is able to clear the bump and spread over the entire domain as shown in Fig. 4a. However, in the case where the maximum height is large, we find that the initial oil drop is not able to clear the bump and gets stuck on it as shown in Fig. 4b. This behavior showcases an inherent limitation of our model in that modelling another liquid as a stationary feature of the surface topography does not allow the "leaky" effects of the surface acoustic wave to be transferred to the moving liquid as it flows over the bump. Essentially, the effect of acoustic driving is lost over the bump region as we consider it to be solid instead of liquid, which is not in acceptance with experimental observations.

5 Conclusion

The presented results show that a reasonably accurate model can be developed for simulating the movement of thin film flows over topography when driven primarily by SAWs. We first develop a governing nonlinear PDE by simplifying the incompressible Navier-Stokes equations for the problem using the lubrication approximation, with a further simplification to reduce our equation to two spatial dimensions instead of three. We then solve the PDE over a domain of interest by discretizing into a system of ODEs, which is then solved using an implicit time stepping scheme. However, a limitation of our model is that it does not realistically model

the interactions between a flowing and stationary liquid as the assumption that the stationary liquid can be modelled as a feature of the surface topography does not take into the account of leakiness of SAWs in liquids.

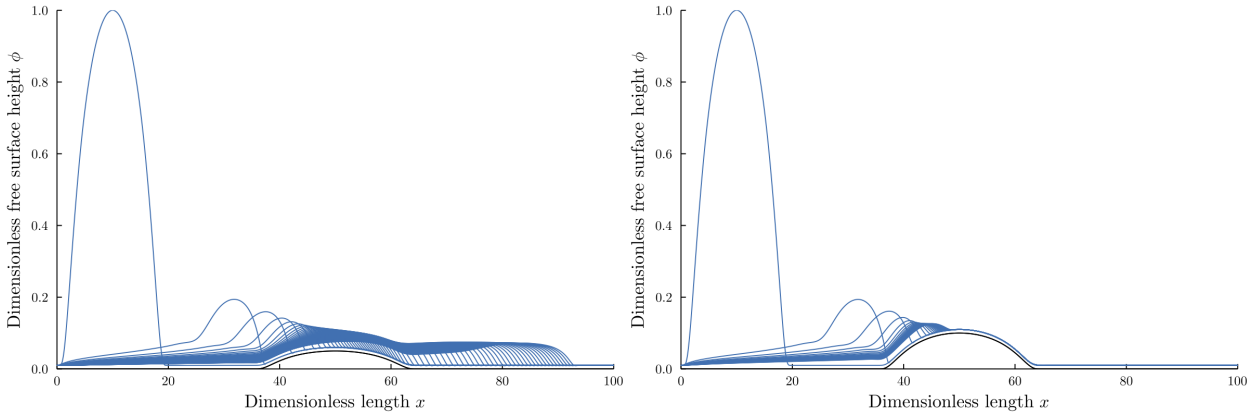

(a) Small bump

(b) Tall bump

Figure 4: Fluid profile on bump topographies plotted every $\Delta t = 10000$ dimensionless time units

Appendices

A Topography Equations

We describe a bump topography by the equation

$$\psi(x) = \begin{cases} he^{-(w^2/(w^2-(x-c)^2))} & x \in (c-w, c+w) \\ 0 & \text{otherwise} \end{cases}$$

where h denotes a scaling factor for the maximum height of the bump, w denotes half the width of the bump, and c denotes the center point of the bump.

B Spatial Discretization Expanded

$$f_j^{(1)} = \frac{1}{2\Delta x^2}\left(\left(h_{j-1}^3 + h_j^3\right)(\phi_{j-1} - \phi_j)) + \left(h_j^3 + h_{j+1}^3\right)(\phi_{j+1} - \phi_j)\right)$$

$$f_j^{(2)} = \frac{1}{2\Delta x^4}\left(\left(h_{j-1}^3 + h_j^3\right)(\phi_{j-2} - 3\phi_{j-1} + 3\phi_j - \phi_{j+1}) + \left(h_j^3 + h_{j+1}^3\right)(-\phi_{j-1} + 3\phi_j - 3\phi_{j+1} + \phi_{j+2})\right)$$

$$f_j^{(3)} = \frac{1}{2\Delta x}\left(h_{j+1}^3 - h_{j-1}^3\right)$$

$$f_j^{(4)} = \frac{1}{2\Delta x}\left(h_{j+1}^3 e^{2k_i x_{j+1}}\left(1 + \alpha_1\varepsilon\left(\frac{\phi_{j+2} - \phi_j}{2\Delta x}\right)\right) - h_{j-1}^3 e^{2k_i x_{j-1}}\left(1 + \alpha_1\varepsilon\left(\frac{\phi_j - \phi_{j-2}}{2\Delta x}\right)\right)\right)$$

References

[AM16] G. Altshuler and O. Manor. "Free films of a partially wetting liquid under the influence of a propagating MHz surface acoustic wave". In: *Physics of Fluids* 28.7 (2016), p. 072102.

[DK02] J. A. Diez and L. Kondic. "Computing three-dimensional thin film flows including contact lines". In: *Journal of Computational Physics* 183.1 (2002), pp. 274–306.

[KBH00] S. Kalliadasis, C. Bielarz, and G. Homsy. "Steady free-surface thin film flows over topography". In: *Physics of Fluids* 12.8 (2000), pp. 1889–1898.

[Kon03] L. Kondic. "Instabilities in gravity driven flow of thin fluid films". In: *Siam review* 45.1 (2003), pp. 95–115.

[SL88] L. E. Stillwagon and R. G. Larson. "Fundamentals of topographic substrate leveling". In: *Journal of Applied Physics* 63.11 (1988), pp. 5251–5258.

[SM94] S. Shiokawa and Y. Matsui. "The Dynamics of SAW Streaming and its Application to Fluid Devices". In: *MRS Proceedings* 360 (1994), p. 53.

[Ver+12] S. Veremieiev, H. Thompson, M. Scholle, Y. C. Lee, and P. Gaskell. "Electrified thin film flow at finite Reynolds number on planar substrates featuring topography". In: *International journal of multiphase flow* 44 (2012), pp. 48–69.

[Ver11] S. Veremieiev. *Gravity-driven continuous thin film flow over topography*. University of Leeds, 2011.